

GLOBAL STREAMING INSTABILITY IN RING-SHAPED PROTOPLANETARY DISKS

MIR ABBAS JALALI

Computational Mechanics Laboratory, Department of Mechanical Engineering
 Sharif University of Technology, Azadi Avenue, P.O. Box: 11155-9567, Tehran, Iran
Submitted to the Astrophysical Journal, January 10, 2013

ABSTRACT

We use the Fokker-Planck equation and model the dispersive dynamics of solid particles in annular protoplanetary disks whose gas component is more massive than the particle phase. We model particle–gas interactions as hard sphere collisions, determine the functional form of diffusion coefficients, and show the existence of global unstable modes in the particle phase. These modes have spiral patterns with the azimuthal wavenumber $m = 1$ and rotate slowly. We show that in ring-shaped disks, solid particles subject to gas drag never fall into the central star and instabilities occur for particles of all sizes. Therefore, planetesimals and planetary cores can be efficiently produced through the accumulation of smaller objects near the peaks of unstable density waves.

Subject headings: methods: numerical, hydrodynamics, instabilities, planets and satellites: formation, planetary systems: protoplanetary disks

1. INTRODUCTION

Protoplanetary disks are multi-phase environments composed of solid particles and molecular gas. The motion of particles is mainly governed by the gravitational forces of the disk material and the central star. Gas molecules feel the pressure gradient as well: for a polytropic isothermal gas, whose density profile monotonically increases towards the central star, the pressure gradient ∇p is always negative. This yields a sub-Keplerian circular velocity and generates headwind on solid particles that move on Keplerian orbits. Solid particles are thus expected to inspiral towards the central star. Although adhesive and electrostatic forces can enhance the clustering of micron-sized particles (Blum & Wurm 2008), centimeter- to meter-size particles seem to inspiral towards (and fall into) the central star sooner than the time scale needed for assembling planetary cores. Therefore, several collective processes like streaming instability (Youdin & Goodman 2005), turbulent vortices induced by Kelvin-Helmholtz instability (Johansen et al. 2006; Bai & Stone 2010a,b) and magnetorotational instability (Johansen et al. 2007, 2011) have been proposed to be responsible for the formation of km-scale planetesimals.

The inspiraling motion of particles, however, does not globally occur in disks with non-monotonic density profiles, which are likely to form through a combination of viscous accretion and photoevaporation by the central star (e.g., Matsuyama et al. 2003). A ring-like disk is the simplest system with non-monotonic density profile. An interesting property of such systems is that ∇p becomes positive in regions where the density profile is rising, and gas molecules move with super-Keplerian velocities. Consequently, solid particles that approximately move on Keplerian orbits are accelerated by gas and migrate outwards. This means that solid particles do not necessarily fall into the central star and may instead migrate into regions where both the head and tail winds are minimized. Possible instabilities triggered by such migrations can have remarkable implications for the for-

mation of planetesimals and planetary cores.

In this paper, we generalize the analysis of Jalali & Tremaine (2012, hereafter JT12) to disks that include a locally isothermal gas component, and search for global instabilities in the particle phase. Our disks are self-gravitating and the particle phase has non-zero radial velocity dispersion. The dynamics of particles is modeled by the Fokker-Planck equation, and the gas component is assumed to be in a steady-state rotation around the central star. For simplicity, we confine our study to disks with $\Sigma_g/\Sigma_p \gg 1$ where Σ_g and Σ_p are the surface densities of the gas and particle phases, respectively. By this assumption, the gas component does not respond to the disturbances of the particle phase. We neglect collisions between solid particles, but those between gas molecules and solid particles are taken into account.

2. DISK MODEL

We assume a two-phase medium consisting of solid particles and gas molecules, and refer to them by subscripts p and g , respectively. Solid particles are assumed to be monodisperse hard spheres of mass m_p and radius r_p . The gas phase has the molecular mass m_g , and the average radius of gas molecules is r_g . We work with initially axisymmetric disks whose gas component has not streaming motion in the radial direction, but particles can move on eccentric orbits. For both the particle and gas phases we use the annular ring model of JT12 whose dimensionless surface density is

$$\Sigma_0(R) = \frac{3\mu}{4\pi} \frac{R^2}{(1+R^2)^{5/2}}, \quad \mu = \frac{M_d}{M_\star}, \quad R = \frac{r}{b}, \quad (1)$$

where $M_d = M_p + M_g$ is the total disk mass, M_\star is the mass of central star, M_p is the mass of particles, M_g is the mass of gas component, b is a length scale, and r is the radial distance to the central star. Figure 1 shows the radial profile of Σ_0/μ that peaks at $R = \sqrt{6}/3$. We suppose that the surface densities of the particle and gas phases are proportional to Σ_0 so that $\Sigma_\nu(R) = \bar{M}_\nu \Sigma_0(R)$ with $\nu \equiv p, g$ and $\bar{M}_\nu = M_\nu/M_d$. Defining G as the gravita-

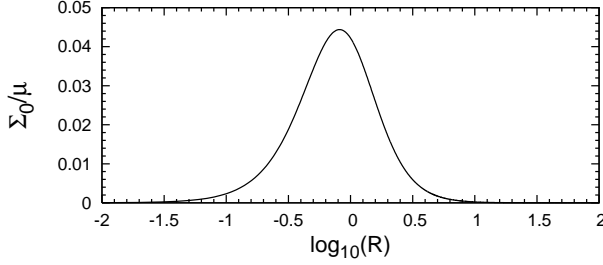


Figure 1. Density profile of ring-shaped disks.

tion constant, the dimensionless total gravitational potential field arising from Σ_0 and the central star becomes

$$V_0(R) = \frac{b\Phi_0}{GM_\star} = -\frac{1}{R} - \frac{\mu}{2} \frac{1+2R^2}{(1+R^2)^{3/2}}, \quad (2)$$

where Φ_0 is the actual potential.

We work with initially axisymmetric disks whose gas component has not streaming motion in the radial direction. If the gas is locally isothermal, its dimensionless pressure will be determined from

$$p = c_s^2 \Sigma_g, \quad c_s^2 = \left(\frac{b}{GM_\star} \right) \left(\frac{k_B T_g}{m_g} \right), \quad (3)$$

where c_s is the normalized sound speed, k_B is the Boltzmann constant, and T_g is the absolute temperature of the gas. In passive disks heated by the stellar radiation (not by accretion), and sufficiently far from the central star, the radial profile of T_g is given by (Armitage 2010, §2.4)

$$T_g = T_\star \left(\frac{r_\star}{2\pi b} \right)^{3/4} \frac{1}{R^{3/4}}, \quad (4)$$

where T_\star is the effective temperature of the central star and r_\star is its radius. The mean thermal speed of gas molecules is related to the sound speed as $v_{\text{th}}^2 = (8/\pi)c_s^2$. We therefore find

$$v_{\text{th}} = \alpha R^{-3/8}, \quad \alpha = \left(\frac{8bk_B T_\star}{\pi GM_\star m_g} \right)^{1/2} \left(\frac{r_\star}{2\pi b} \right)^{3/8}. \quad (5)$$

In the solar system, with b set to Jupiter's orbital semi-major axis, and m_g being the molecular mass of H_2 , one obtains $\alpha \approx 0.022$. For Fomalhaut's ring with $b \approx 140\text{AU}$ and for the inner ring of AB Aurigae with $b \approx 40\text{AU}$ (Hashimoto et al. 2011), we find $\alpha \approx 0.036$ and 0.026 , respectively.

In the absence of collisions between solid particles and gas molecules, the velocity of solid particles on circular orbits is determined from

$$v_{\text{p},c}^2 = R \frac{dV_0}{dR} = \frac{1}{R} + \frac{\mu}{2} \frac{R^2(2R^2-1)}{(1+R^2)^{5/2}}, \quad (6)$$

and the radial momentum equation for the gas becomes

$$-\Sigma_g \frac{v_{\text{g},c}^2}{R} = -\frac{dp}{dR} - \Sigma_g \frac{dV_0}{dR}, \quad (7)$$

from which we obtain the circular velocity of gas:

$$v_{\text{g},c}^2 = \frac{5\pi}{24} \frac{(1-3R^2)}{(1+R^2)} v_{\text{th}}^2 + v_{\text{p},c}^2. \quad (8)$$

The condition $v_{\text{p},c}^2 \geq 0$ implies $\mu \leq 5^{5/2}$, which is satisfied by protoplanetary disks. It is seen that for $R^2 < 1/3$, the gas streaming velocity exceeds the speed of particles and generates tailwind on them. This is a remarkable and largely overlooked feature of ring-shaped disks, and has interesting implications for the dynamics of solid particles in protoplanetary disks: while particles experience a resistive headwind for $R^2 > 1/3$ and inspiral towards the central star, they are accelerated when $R^2 < 1/3$ and migrate outwards. Inward and outward migrating particles will then be accumulated around $R^2 \approx 1/3$, but this is not the whole story. In next sections we show that global exponentially growing instabilities accompany such radial migrations.

3. EVOLUTIONARY DYNAMICS OF SOLID PARTICLES

The dynamics of particles is described by the phase space distribution function (DF) $f(\mathbf{x}, \mathbf{v}, t) = m_p \mathcal{N}_p(\mathbf{x}, \mathbf{v}, t)$ where \mathcal{N}_p is the number density of particles. The vectors $\mathbf{x} = (x_1, x_2)$ and $\mathbf{v} = (v_1, v_2)$ (both in Cartesian coordinates) are the position and velocity vectors of particles in the disk plane, and t is the time. We utilize the DF (Jalali & Tremaine 2012, §3)

$$f_0 = m_p \mathcal{N}_{p,0} = L^{2K+2} g_K(E), \quad (9)$$

to model the initial distribution of particles, before turning on the collisions between solid particles and gas molecules. Here $L = |\mathbf{x} \times \mathbf{v}|$ and $E = \frac{1}{2} \mathbf{v} \cdot \mathbf{v} + V_0$ are, respectively, the orbital angular momentum and energy of particles per unit mass. K is a positive integer that controls the mean eccentricity \bar{e} of the disk. The function $g_K(E)$ takes physical (positive) values for $K \geq 2$, and \bar{e} decreases as K is increased. In the limit of $K \rightarrow \infty$ the disk becomes cold with all particles moving on circular orbits.

In this study we ignore particle-particle collisions, and assume that colliding solid particles and gas molecules are hard spheres. The evolution of f is therefore expressed by the Fokker-Planck equation (Binney & Tremaine 2008, §7.4)

$$\begin{aligned} \frac{\partial f}{\partial t} + v_i \frac{\partial f}{\partial x_i} + a_i \frac{\partial f}{\partial v_i} = & -\frac{\partial}{\partial v_i} (D[\Delta v_i] f) \\ & + \frac{1}{2} \frac{\partial^2}{\partial v_i \partial v_j} (D[\Delta v_i \Delta v_j] f), \end{aligned} \quad (10)$$

where $D[\Delta v_i]$ and $D[\Delta v_i \Delta v_j]$ are diffusion coefficients and a_i are the components of the acceleration vector. In equation (10) and throughout the paper a repeated integer index stands for summation over that index from 1 to 2. The acceleration vector is computed from $\mathbf{a} = -\nabla V = -\nabla[V_0 + V_1(R, \phi, t)]$ where the perturbed potential V_1 is self-consistently calculated from the density disturbance $\Sigma_1(R, \phi, t)$ of particle distribution. Since we have assumed $\Sigma_p \ll \Sigma_g$, the contribution of the gas component to V_1 is neglected.

For local collisions, the diffusion coefficients are evaluated using the procedure of Rosenbluth et al. (1957), but for three dimensional collisions of hard spheres with the cross section $\sigma = \beta^2/4$ where $\beta = r_p + r_g$. Let us define $\gamma = m_g/(m_p + m_g)$ and denote the absolute velocity of

gas molecules by \mathbf{v}' . We obtain

$$D[\Delta v_i] = \frac{\partial h(\mathbf{x}, \mathbf{v}, t)}{\partial v_i}, \quad D[\Delta v_i \Delta v_j] = \frac{\partial^2 g(\mathbf{x}, \mathbf{v}, t)}{\partial v_i \partial v_j}, \quad (11)$$

where the potential functions $h(\mathbf{x}, \mathbf{v}, t)$ and $g(\mathbf{x}, \mathbf{v}, t)$ are given by the following integrals

$$h = \frac{-\pi\gamma\beta^2}{3} \int \mathcal{N}_g(\mathbf{x}, \mathbf{v}', t) |\mathbf{v} - \mathbf{v}'|^3 d\mathbf{v}', \quad (12)$$

$$g = \frac{\pi\gamma^2\beta^2}{15} \int \mathcal{N}_g(\mathbf{x}, \mathbf{v}', t) |\mathbf{v} - \mathbf{v}'|^5 d\mathbf{v}', \quad (13)$$

and $\mathcal{N}_g(\mathbf{x}, \mathbf{v}', t)$ is the number density of gas molecules in the phase space. Defining

$$[\Sigma_p, \Sigma_p \bar{v}_i, \Sigma_p \bar{v}_i \bar{v}_j] = \int [1, v_i, v_i v_j] f d\mathbf{v}, \quad (14)$$

the elements of the stress tensor are determined as $\tau_{ij} = \Sigma_p (\bar{v}_i \bar{v}_j - \bar{v}_i \bar{v}_j)$. The macroscopic quantities Σ_p , \bar{v}_i and τ_{ij} are functions of \mathbf{x} and t , and the second term on the right-hand side of equation (10) integrates to zero up to the first-order moment equations. Collisional terms involving $g(\mathbf{x}, \mathbf{v}, t)$ correspond to random motions, and contribute to the evolutionary equations of τ_{ij} (second-order moments of the Fokker-Planck equation). We neglect them in the present study because the mass ratio of gas molecules to solid particles is small, $m_g/m_p \ll 1$, which implies $g/h \sim \mathcal{O}(m_g/m_p)$. The Fokker-Planck equation can therefore be reduced to

$$\frac{\partial f}{\partial t} + \frac{\partial}{\partial x_i} (\dot{x}_i f) + \frac{\partial}{\partial v_i} (\dot{v}_i f) = 0, \quad (15)$$

with

$$\dot{x}_i = v_i, \quad \dot{v}_i = -\frac{\partial V}{\partial x_i} + D[\Delta v_i]. \quad (16)$$

Differentiating (12) with respect to v_i gives

$$D[\Delta v_i] = -\pi\gamma\beta^2 \int \mathcal{N}_g(\mathbf{x}, \mathbf{v}', t) |\mathbf{v} - \mathbf{v}'| (v_i - v'_i) d\mathbf{v}'. \quad (17)$$

Evaluating this integral requires the explicit form of \mathcal{N}_g , which can be modeled (for example) by a Maxwell-Boltzmann distribution. Nonetheless, such details are not necessary if we make some further simplifying assumptions: Let $(\mathbf{e}_R, \mathbf{e}_\phi)$ be unit base vectors in the polar coordinates (R, ϕ) , and $e \ll 1$ denote the orbital eccentricity of particles. The velocities of particles and gas molecules will be approximated as

$$\mathbf{v} \sim v_{p,c} \mathbf{e}_\phi + \mathcal{O}(eR\Omega), \quad \mathbf{v}' \sim v_{g,c} \mathbf{e}_\phi + \mathcal{O}(v_{th}), \quad (18)$$

where $\Omega = R^{-3/2} + \mathcal{O}(\mu)$ is the orbital frequency of particles. We think of disks with $v_{th} < v_{p,c}, v_{g,c}$ over $0.032 \lesssim R \lesssim 10$ (cf. Figure 1) to guarantee the existence of bound orbits, and avoid gas dispersal through photoevaporation. The mean eccentricity corresponding to (9) is almost constant over the entire disk space (see JT12), and it is given by $\bar{e} = [\pi/(4K+2)]^{1/2} + \mathcal{O}(\mu)$. For $\alpha \sim \mathcal{O}(10^{-2})$, which corresponds to protoplanetary disks around solar-type stars, and for $K \leq 29$ experimented in JT12, one has

$$\bar{e} \gg \frac{v_{th}}{R\Omega} = \alpha R^{1/8} + \mathcal{O}(\mu), \quad 0.032 \leq R \leq 10. \quad (19)$$

From (8), (18) and (19) we conclude that the bulk of particles satisfy $|\mathbf{v} - \mathbf{v}'| \approx eR\Omega$, and the integral in (17) is approximated by

$$D[\Delta v_i] \approx -\xi_0 eR\Omega \rho_g (v_i - U_i), \quad (20)$$

$$\xi_0 = \pi \left(\frac{M_\star}{m_p} \right) \left(\frac{r_p}{b} \right)^2, \quad (21)$$

where $\rho_g = \Sigma_g(R)\delta(z)$ is the spatial gas density normalized to M_\star/b^3 , and $U_i(\mathbf{x}, t) = \bar{v}'_i$ are the streaming velocity components for the gas. $\delta(z)$ is the Dirac delta function. It is remarked that all velocities are normalized to $[GM_\star/b]^{1/2}$. To trace the evolution of particles in the disk plane, we soften $\delta(z)$ using its Poisson kernel as $\delta_\epsilon(z) = \pi^{-1}\epsilon/(\epsilon^2 + z^2)$ and evaluate $D[\Delta v_i]$ at $z = 0$. The small parameter ϵ determines the vertical size of the disk. With $\epsilon = r_p/b$ the scattering of gas molecules takes place in the disk plane and the cross section σ becomes a line of the length $r_p + r_g$. For near-circular orbits with $e \rightarrow 0$, one obtains $|\mathbf{v} - \mathbf{v}'| \approx v_{th}$ and $D[\Delta v_i]$ transforms to the well-known form of Epstein drag.

Solving (15) in a four-dimensional phase space, with particle motions confined to the disk plane, is facilitated by utilizing the angle variables $\mathbf{w} = (w_1, w_2)$ and their conjugate actions $\mathbf{J} = (J_1, J_2)$. We follow JT12 and set J_1 and J_2 to the radial action and the orbital angular momentum Rv_ϕ , respectively. In the (\mathbf{w}, \mathbf{J}) -space, the motion equations (16) become

$$\dot{w}_i = \frac{\partial \mathcal{H}}{\partial J_i} - F_{J_i}, \quad \dot{J}_i = -\frac{\partial \mathcal{H}}{\partial w_i} + F_{w_i}, \quad i = 1, 2, \quad (22)$$

where $\mathcal{H} = \frac{1}{2}\mathbf{v} \cdot \mathbf{v} + V(\mathbf{x}, t)$ is the Hamiltonian function, and the functions F_{J_i} and F_{w_i} are determined using the virtual work of nonconservative forces:

$$F_{w_i} \delta w_i + F_{J_i} \delta J_i = D[\Delta v_i] \cdot \delta x_i, \quad (23)$$

with δ being the variational operator. After expanding $D[\Delta v_i]$ and δx_i in Fourier series of angle variables, we obtain $F_{w_i}(\mathbf{J}, w_1)$ and $F_{J_i}(\mathbf{J}, w_1)$, which are real harmonic functions of w_1 and are smooth in the \mathbf{J} -space. We now write equation (15) in the angle-action space:

$$\frac{\partial f}{\partial t} + [f, \mathcal{H}] + \mathcal{D}_F f = 0, \quad (24)$$

where $[\cdot, \cdot]$ denotes the Poisson bracket over the (\mathbf{w}, \mathbf{J}) -space and the operator \mathcal{D}_F is defined by

$$\mathcal{D}_F = \frac{\partial F_{w_i}}{\partial J_i} - \frac{\partial F_{J_i}}{\partial w_i} + F_{w_i} \frac{\partial}{\partial J_i} - F_{J_i} \frac{\partial}{\partial w_i}. \quad (25)$$

4. UNSTABLE MODES

We seek solutions of the form $f = f_0(\mathbf{J}) + f_1(\mathbf{w}, \mathbf{J}, t)$ for equation (24) so that $|f_1| \ll |f_0|$. The Hamiltonian corresponding to f will become $\mathcal{H} = \mathcal{H}_0 + V_1$ where the perturbed potential V_1 (self-consistently arising from f_1) and $\mathcal{H}_0 = \frac{1}{2}\mathbf{v} \cdot \mathbf{v} + V_0(R)$ are expressed in the angle-action space (Jalali 2010, §2). f_1 is obtained by solving the linearized Fokker-Planck equation:

$$\frac{\partial f_1}{\partial t} + [f_1, \mathcal{H}_0] + [f_0, V_1] + \mathcal{D}_F f_1 = -\mathcal{D}_F f_0, \quad (26)$$

which is a non-homogenous partial differential equation. The particular solution of (26) is a steady drift of the

Table 1
Pattern speeds and growth rates of slow modes A1 and A2 versus ξ .

ξ	Mode A1		Mode A2	
	$\omega_r \times 10^3$	$s \times 10^5$	$\omega_r \times 10^3$	$s \times 10^5$
0	5.172	0	4.944	0
0.04	5.172	1.203	4.944	1.631
0.12	5.175	3.613	4.942	4.887
0.20	5.181	6.036	4.939	8.127
0.28	5.190	8.471	4.936	11.34
0.36	5.201	10.91	4.932	14.51
0.50	5.225	15.18	4.927	19.75

form $f_d(\mathbf{J}, w_1)$ that satisfies

$$[f_d, \mathcal{H}_0] + [f_0, V_d] + \mathcal{D}_F f_d = -\mathcal{D}_F f_0, \quad (27)$$

where the potential V_d corresponds to f_d . We are interested in non-axisymmetric solutions that depend on (w_1, w_2) and t . For a slowly rotating density wave $\Sigma_1(R, \phi, t) = \text{Re} \int f_1 d\mathbf{v}$ with the azimuthal wavenumber m , we consider unsteady DFs of the form (JT12, §6) $f_1 = \tilde{f}_1(\mathbf{J}) \exp[-i\omega t + im(w_2 - w_1)]$ and compute the eigenfrequency $\omega = \omega_r + is$ and \tilde{f}_1 through solving the homogeneous part of equation (26). Here ω_r and s are, respectively, the pattern speed and growth/decay rate of density perturbations. We formulate the eigenvalue problem following the finite element method of Jalali (2010) and JT12, and compute the eigenfrequency spectrum of $m = 1$ waves for a model with $K = 29$, $\alpha = 0.025$, $\mu = 0.08$, and $M_p/M_g = 1/8$, and for several choices of $\xi = \xi_0/(\pi\epsilon)$. The mean eccentricity of particle orbits of this model is $\bar{e} = 0.156$. Our finite element model has $N = 180$ ring elements whose radial nodes are located at $R_n = 10^{(4n-2N-4)/(N+1)}$ for $n = 1, 2, \dots, N$. Using this mesh, eigenfrequencies are calculated with a relative accuracy $\leq 0.1\%$.

In the absence of gas drag, $\xi = 0$, the spectrum contains only two stable slow modes, which are labelled by A1 and A2. The pattern speeds of these modes satisfy the inequality $\omega_r > \Omega_{\text{pr,max}} = 0.00469$ where $\Omega_{\text{pr}} = \Omega_2 - \Omega_1$ is the precession frequency of particle orbits. The orbital frequencies $\Omega_i = \partial\mathcal{H}_0/\partial J_i$ ($i = 1, 2$) are calculated in the unperturbed state. All other modes are singular and form a continuum over the range $\Omega_{\text{pr,min}} < \omega_r < \Omega_{\text{pr,max}}$. By setting $\xi > 0$ and turning on the gas drag, all singular and long-wavelength modes become unstable. The pattern speeds and growth rates of modes A1 and A2 have been reported in Table 1 for several values of ξ . Assuming that the mass of each particle is computed from $m_p = (4/3)\pi\rho_s r_p^3$, with ρ_s being the typical density of rocky material, one finds $\xi \propto 1/r_p$. Therefore, instability-induced accumulation of smaller particles happens faster.

As Table 1 shows, mode A2 grows faster than mode A1 but it rotates slower. Gas drag has not a notable contribution to the pattern speeds of modes and it only controls the growth rate so that s linearly increases in terms of ξ . Figure 2 displays the perturbed density patterns of stable and unstable modes. It is evident that these modes are confined to the region with rising density profile. We find that the spirality of mode A1 increases proportional to ξ . Comparing the modal content of our

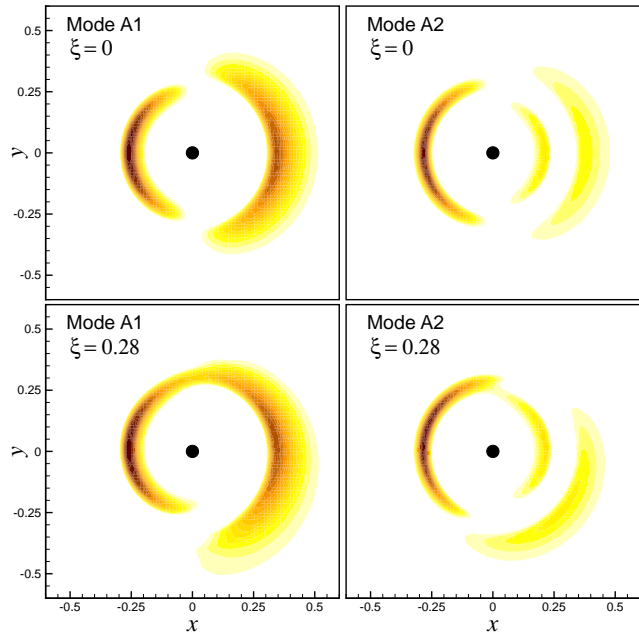


Figure 2. Mode shapes of global stable (*top*) and unstable (*bottom*) density waves of the particle phase in a protoplanetary disk with $\mu = 0.08$, $M_p/M_g = 1/8$ and $\bar{e} = 0.156$. The parameter ξ is equal to 0 and 0.28 for stable and unstable modes, respectively. Contour plots show the positive parts of the perturbed density Σ_1 at $t = 0$. Unstable mode A1 is a trailing spiral while the wave packets of unstable mode A2 form a leading pattern. Filled circle shows the location of the central star.

$\xi = 0$ disks with the results of JT12 (see their Figure 4) shows that short-wavelength slow modes have been disappeared by setting $M_p < M_d$ and the pattern speeds of the modes with the longest wavelengths have approached to $\Omega_{\text{pr,max}}^+$. This is very similar to the behavior of disk galaxies: increasing the mass of dark matter halo stabilizes tightly wound spiral modes and only modes with the longest wavelengths, especially the bar mode, survive (Jalali 2007). The number of slow modes also depends on the mean eccentricity of particle orbits. Our numerical experiments show that mode A2 disappears as its pattern speed drops well below $\Omega_{\text{pr,max}}$ by increasing \bar{e} .

Using equation (27) one can show that the particle distribution has a secular increase towards $R^2 \approx 1/3$ so that $f_d(a, e, w_1) \sim \mathcal{O}(\eta w_1/\Omega_1) \sim \mathcal{O}(\eta t)$ where $\eta = \xi \bar{e} a \Omega(a) \Sigma_g(a)$, and a is the instantaneous semi-major axis of a test particle's orbit. At $R = \sqrt{6}/3$ where the particle density is maximum we have $\eta \approx 5 \times 10^{-4} \xi$, which has the same order of magnitude of s . We conclude that since instabilities grow exponentially as $f_1 \sim \mathcal{O}(e^{st})$, they will overwhelm the particle accumulation induced by radial drift.

5. DISCUSSIONS

The infall time scale of $\mathcal{O}(10^2)$ yr for meter-sized solid bodies puts a strong constraint on the formation of planetesimals from dust grains and pebbles (Weidenschilling 1977). Recent simulations have shown that the backreaction of particles on gas can trigger out-of-plane Kelvin-Helmholtz instability, which boosts local particle density and helps self-gravity to assemble km-size bodies. Turbulence, on the other hand, imposes stochastic forces on planetesimals, increases their collision frequency and

disrupts those with ≤ 10 km radius (Nelson & Gressel 2010). Although the random forcing of planetesimals can be suppressed in the presence of a dead zone (Gressel et al. 2011), alternative and simpler processes may also be involved in the formation of super km-scale planetesimals.

Slow density waves exist in all near-Keplerian, self-gravitating rings and can be excited by encounters (JT12). Addition of a gas component, however, destabilizes the particle phase without any external disturbance. We showed that the drag-induced infall of solid bodies into the central star is not a universal phenomenon and the direction of particle migration highly depends on the disk structure. There will be no infall if at some region the disk density profile, including its solid particle and gas components, rises outwards. Therefore, with a preserved source of solid particles in the disk, global instabilities explored in this study will have time to boost the particle density to arbitrarily large levels and enhance the formation of bigger objects through gravitational collapse.

Our results have been obtained for self-gravitating disks whose particle phase is constituted from monodisperse hard spheres. Including the size distribution of particles and the effect of particle-particle collisions, especially catastrophic disruptions, is an interesting problem for future studies. Moreover, by assuming $\Sigma_p \ll \Sigma_g$ we neglected the backreaction of particles on gas flow. Generalization of our study to disks with $\Sigma_p \gtrsim \Sigma_g$ requires simultaneous solution of hydrodynamic and Fokker-Planck

equations. In such circumstances, we anticipate effective angular momentum exchange between the particle and gas phases, and the gas phase may also become unstable.

I thank Scott Tremaine for his stimulating discussions and useful comments.

REFERENCES

- Armitage P.J., 2010, *Astrophysics of Planet Formation*, Cambridge University Press, Cambridge
- Binney J., Tremaine S., 2008, *Galactic Dynamics*, 2nd edition, Princeton University Press, Princeton
- Blum J., Wurm G., 2008, *ARA&A*, 46, 21
- Gressel O., Nelson R.P., Turner N.J., 2011, *MNRAS*, 415, 3291
- Hashimoto J. et al., 2011, *ApJ*, 729, L17
- Johansen A., Klahr H., Henning Th., 2006, *ApJ*, 636, 1121
- Johansen A., Oishi J.S., Mac Low M.-M., Klahr H., Henning Th., Youdin A., 2007, *Nature*, 448, 1022
- Johansen A., Klahr H., Henning Th., 2011, *A&A*, 529, A62
- Bai X.-N., Stone J.M., 2010a, *ApJS*, 190, 297
- Bai X.-N., Stone J. M., 2010b, *ApJ*, 722, 1437
- Jalali M.A., 2007, *ApJ*, 669, 218
- Jalali M.A., 2010, *MNRAS*, 404, 1519
- Jalali M.A., Tremaine S., 2012, *MNRAS*, 421, 2368
- Matsuyama I., Johnstone D., Hartmann L., 2003, *ApJ*, 582, 893
- Nelson R. P., Gressel O., 2010, *MNRAS*, 409, 639
- Rosenbluth M.N., MacDonald W.M., Judd D.L., 1957, *Physical Review*, 107, 1
- Weidenschilling S. J., 1977, *MNRAS*, 180, 57
- Youdin A.N., Goodman J., 2005, *ApJ*, 620, 459